Communication

Cucurbit[7]uril Induces Superior Probe Performance for Single-Molecule Detection

Tami A. Martyn, Jason L. Moore, Ronald L. Halterman, and Wai Tak Yip

J. Am. Chem. Soc., **2007**, 129 (34), 10338-10339• DOI: 10.1021/ja073996n • Publication Date (Web): 04 August 2007

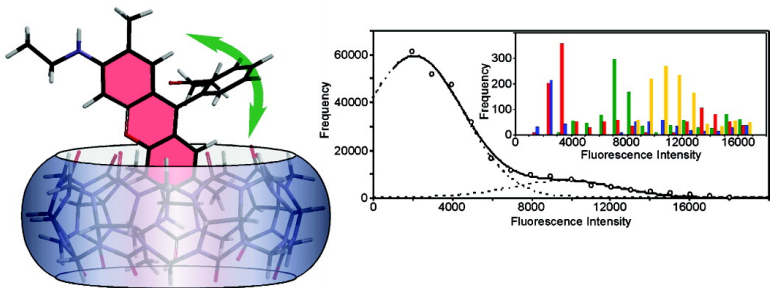

More About This Article

Additional resources and features associated with this article are available within the HTML version:

- Supporting Information
- Links to the 1 articles that cite this article, as of the time of this article download
- Access to high resolution figures
- Links to articles and content related to this article
- Copyright permission to reproduce figures and/or text from this article

View the Full Text HTML

J|A|C|S
COMMUNICATIONS

Published on Web 08/04/2007

Cucurbit[7]uril Induces Superior Probe Performance for Single-Molecule Detection

Tami A. Martyn, Jason L. Moore, Ronald L. Halterman, and Wai Tak Yip*

Department of Chemistry and Biochemistry, University of Oklahoma, Norman, Oklahoma 73019

Received June 1, 2007; E-mail: ivan-yip@ou.edu

Single-molecule spectroscopy (SMS) is a powerful technique for studying molecular dynamics in fluorophore-labeled biomolecules and macromolecules. Because of their small size, broad spectral coverage, diverse conjugation scheme, and high fluorescence quantum efficiency, organic fluorophores have been widely used in SMS. Unfortunately, poor photostability renders most incompatible to applications that require prolonged fluorescence tracking. Thus, small, bright, and long-lasting fluorophores are being actively pursued. Notable examples include relatively large dye-doped silica nanoparticles and semiconducting nanoparticles.[1] Although they exhibit desirable photophysical properties, their disadvantage in size has yet to be fully overcome. A more promising approach would be to retain the advantages of organic fluorophores by including them in a host that would enhance their fluorescence intensity and photostability without increasing their size significantly. Herein, we report the dual functions of cucurbit[7]uril (CB7) to enhance the performance of rhodamine 6G (R6G) as a fluorescent probe and to effectively immobilize R6G molecules on glass substrates for SMS.

Recently, CB7 has been shown to enhance the brightness and photostability of organic fluorophores in ensemble measurements.[2,3] As a macrocyclic host, CB7 (Figure 1) has a center cavity that exhibits a strong affinity toward cationic molecules.[4] Organic fluorophores like R6G have been shown to bind strongly to CB7 with a binding constant exceeding 50 000 M^{-1}.[5] Unlike nanoparticles, a CB7/fluorophore complex is only slightly bigger than, and is expected to inherit the same degree of conjugation diversity from, the fluorophore itself, allowing its use even in small molecules with little perturbation. Despite multiple advantages, fluorescence enhancement by CB7 has to the best of our knowledge never been studied at the single-molecule level.

Synthesis of CB7 was adapted from the literature.[6] Typically a sample for SMS was prepared by drying 50 μL of 0.1 mM aqueous CB7 solution on a clean coverglass at 50 °C, which leaves behind a ragged lamina of CB7 on the glass surface. The CB7 lamina was then presented to a 100 nM aqueous R6G solution for 1 min before the sample was rinsed three times with Millipore water to wash away excess CB7 and uncomplexed R6G. After purge drying by nitrogen, no discernible trace of ragged CB7 lamina could be identified by visual inspection. All samples were then examined by a home-built raster scanning confocal microscope.[7]

Our data indicate that the enhancement of R6G fluorescence and photostability persists at the single CB7/R6G complex level. We also noticed that CB7 provides additional interactions to immobilize R6G onto a pristine glass surface, presumably because of H-bonding between the peripheral carbonyl groups of CB7 and the silanol groups on the glass surface. Figure 1A indicates that freshly prepared samples remain hydrated and that free R6G diffuses rapidly on the wet surface while the image is being collected, leaving numerous horizontal streaks in the resultant fluorescence image.[8] On the other hand, the CB7/R6G complex appears stationary in Figure 1B, producing discrete fluorescence spots on a background that is mostly devoid of fluorescence streaking. The strong

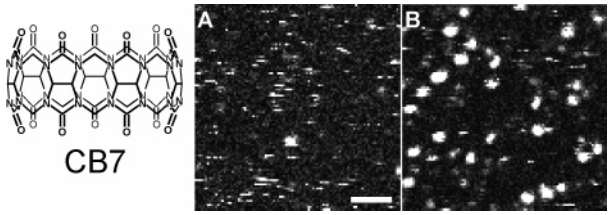

Figure 1. Molecular structure of CB7 and fluorescence images of (A) R6G alone and (B) CB7/R6G on coverglasses. Scale bar is 2 μm.

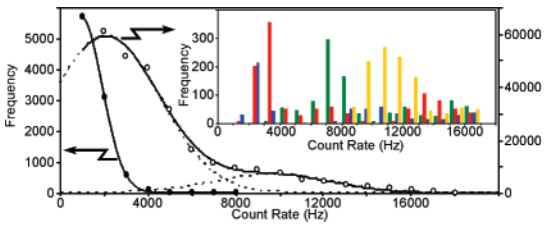

Figure 2. Emission rate histogram of 103 R6G molecules (●), 219 CB7/R6G complexes (○), and 4 individual CB7/R6G complexes (inset). Dashed lines are Gaussian fittings to the emission-rate distributions.

interactions between CB7 and glass are reflected by the high number density of immobilized fluorescence spots as opposed to that in Figure 1A. This is in stark contrast to ref 5 where higher long-term storage stability in CB7/R6G was attributed to reduced surface adsorption. A plausible explanation is that while CB7 helps immobilize R6G, it enhances stability by blocking all extensive contacts between R6G and glass that facilitate photo- and thermal degradations.[9] The fluorescence spots above also suggest that emission from CB7/R6G is consistently brighter than R6G alone, demonstrating the fluorescence enhancement ability of CB7 on R6G upon complex formation. This fluorescence enhancement is not due to a faster radiative relaxation of R6G, but has been attributed to the shielding of R6G from solvent induced nonradiative relaxations by CB7 in the form of a CB7/R6G inclusion complex.[2]

The fluorescence intensity histograms constructed from single molecules of CB7/R6G and R6G were also compared. To afford higher immobilization efficiency, we trapped free R6G inside a 5-bilayer polyelectrolyte/silica hybrid film instead of depositing R6G directly onto a coverglass. Our instrument recorded an average signal of 950 Hz and a maximum of no more than 6000 Hz from R6G, whereas CB7/R6G delivered brighter emission under similar excitation intensity, with some molecules reaching 17 000 Hz. Closer inspection on the intensity histogram of CB7/R6G in Figure 2 reveals a bimodal distribution with emission rates centering around 2070 and 9700 Hz, respectively. Both emission rates are higher than that of R6G alone at 950 Hz.

The peak widths in the intensity histograms also indicate that there is a wider distribution of emission intensity in CB7/R6G relative to R6G alone, suggesting that CB7/R6G may also experience richer dynamics. The internal cavity of CB7 is 7.3 Å at the equator and 5.4 Å at both carbonyl portals, which is not big enough to accommodate an entire R6G molecule side-on.[10] As a result,

10.1021/ja073996n CCC: $37.00

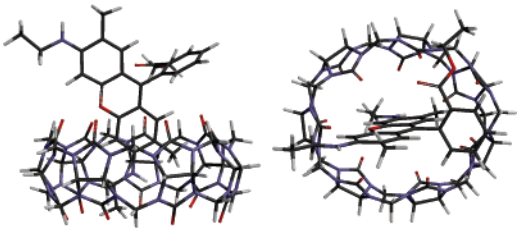

Figure 3. Side and top views of an AM1 geometry optimized CB7/R6G inclusion complex.

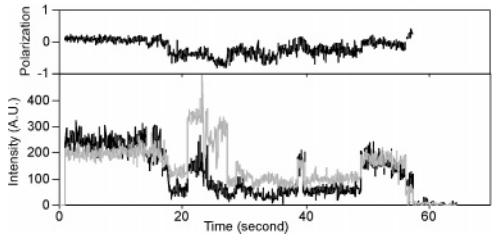

Figure 4. Polarization resolved emission from a CB7/R6G molecule (lower trace) and the corresponding emission polarization (upper trace).

only part of the xanthene moiety would be protected by CB7. This is illustrated qualitatively in an AM1 geometry optimized CB7/R6G complex shown in Figure 3.[11] Presumably, the imperfect fitting of a T-shaped R6G molecule into CB7 prevents the formation of a stable inclusion complex. This may lead to a wide range of complex conformations and therefore a broader peak width in the fluorescence intensity histogram. Accordingly, the bimodal intensity distribution suggests that there are two relatively stable conformations in CB7/R6G, possibly with the better protected R6G fluorescing at a higher emission rate. A less likely alternative is that CB7 and R6G may form an exclusion complex with high enough conformational flexibility to account for the broad peak width and bimodal intensity distribution.[12]

Upon further examinations, we discovered that the wide range of fluorescence intensity is not exclusively caused by a multitude of static CB7/R6G conformations. Instead, Figure 2 inset reveals that the same behavior persists at the single-molecule level. Here, in addition to a higher emission rate than R6G alone, several of the individual CB7/R6G complexes shown display more than one distinct emission rate. This implies that the CB7/R6G complexes were adopting multiple conformations during the course of a measurement. If conformational changes would result in new R6G orientations, emission polarization measurements could be employed to reveal those microscopic motions. In Figure 4 we show a CB7/R6G molecule that emits at several intensity levels. The corresponding changes in emission polarization suggest that intensity variations are frequently accompanied by changes in R6G orientations.[7] This clearly indicates that dynamic conformational fluctuations are partly responsible for the broad intensity distribution found in CB7/R6G. Unlike spectral diffusion where intensity variations are related to spectral shift induced by environmental fluctuations,[13] intensity variations in CB7/R6G are most likely due to changes in fluorescence enhancement directly related to conformational changes.

Ensemble measurements have already confirmed the higher photostability of many CB7/fluorophore complexes relative to the respective fluorophores. For instance, CB7/R6G was reported to be ~1.5 and 30 fold more stable than R6G alone in borosilicate vials at low and high levels of irradiation, respectively.[5] Our single-molecule measurements at low irradiance also reveal a substantial improvement in photostability. The histograms in Figure 5 indicate that both polyelectrolyte/silica hybrid film-embedded R6G and CB7/R6G display a biexponential decay in survival lifetime, which can be attributed to the effect of local heterogeneity commonly revealed by SMS. The averaged survival lifetime $\langle\tau\rangle$ of CB7/R6G is about

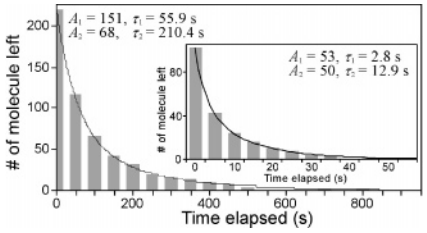

Figure 5. Survival lifetime histograms of CB7/R6G and polyelectrolyte/silica hybrid film-embedded R6G (inset). Solid lines are biexponential decay fittings to the histograms using $y = A_1e^{-t/\tau_1} + A_2e^{-t/\tau_2}$.

13-fold longer than that of R6G alone. The 1.5 fold improvement reported in previous measurements is likely due to interference from uncomplexed, less photostable R6G molecules. In addition, the higher propensity of photodegradation for surface immobilized, as opposed to free, R6G helps widen the difference in photostability further.

In summary, the photophysics of single CB7/R6G molecules have been investigated by a novel immobilization strategy that is based on the strong H-bonding between CB7 and a glass surface. This strategy is particularly attractive in studying cationic fluorophores because of the special affinity of CB7. The CB7/R6G complex displays two stable conformations with different degrees of fluorescence enhancement. Measurements on single CB7/R6G molecules at low irradiance also registered a slightly higher photostability than previous reports obtained from ensemble measurements. Our results suggest that CB7/fluorophore is a superior probe than the fluorophore itself for SMS. Moreover, the combination of small size and potential for conjugation diversity provide a competitive edge for this inclusion complex over other probe technologies currently being developed.

Acknowledgment. This work was supported by NSF-IC (Grant CHE-0442151). R.L.H. thanks the support by the University of Oklahoma Research Council. J.L.M. acknowledges the USDOEd for a GAANN Fellowship.

Supporting Information Available: Additional data for R6G and CB7/R6G. This material is available free of charge via the Internet at http://pubs.acs.org.

References

(1) (a) Santra, S.; Zhang, P.; Wang, K. M.; Tapec, R.; Tan, W. H. *Anal. Chem.* **2001**, *73*, 4988−4993. (b) Bruchez, M.; Moronne, M.; Gin, P.; Weiss, S.; Alivisatos, A. P. *Science* **1998**, *281*, 2013−2016. (c) Chan, W. C. W.; Nie, S. M. *Science* **1998**, *281*, 2016−2018.

(2) Nau, W. M.; Mohanty, J. *Int. J. Photoenergy* **2005**, *7*, 133−141.

(3) Koner, A. L.; Nau, W. M. *Supramol. Chem.* **2007**, *19*, 55−66.

(4) Liu, S. M.; Ruspic, C.; Mukhopadhyay, P.; Chakrabarti, S.; Zavalij, P. Y.; Isaacs, L. *J. Am. Chem. Soc.* **2005**, *127*, 15959−15967.

(5) Mohanty, J.; Nau, W. M. *Angew. Chem., Int. Ed.* **2005**, *44*, 3750−3754.

(6) Day, A.; Arnold, A. P.; Blanch, R. J.; Snushall, B. *J. Org. Chem.* **2001**, *66*, 8094−8100.

(7) Viteri, C. R.; Gilliland, J. W.; Yip, W. T. *J. Am. Chem. Soc.* **2003**, *125*, 1980−1987.

(8) Bardo, A. M.; Collinson, M. M.; Higgins, D. A. *Chem. Mater.* **2001**, *13*, 2713−2721.

(9) Eggeling, C.; Widengren, J.; Rigler, R.; Seidel, C. A. M. *Anal. Chem.* **1998**, *70*, 2651−2659.

(10) (a) Lagona, J.; Mukhopadhyay, P.; Chakrabarti, S.; Isaacs, L. *Angew. Chem., Int. Ed.* **2005**, *44*, 4844−4870. (b) Kim, J.; Jung, I. S.; Kim, S. Y.; Lee, E.; Kang, J. K.; Sakamoto, S.; Yamaguchi, K.; Kim, K. *J. Am. Chem. Soc.* **2000**, *122*, 540−541.

(11) (a) Wang, R. B.; Yuan, L.; Macartney, D. H. *Chem. Commun.* **2005**, 5867−5869. (b) Sindelar, V.; Cejas, M. A.; Raymo, F. M.; Kaifer, A. E. *New J. Chem.* **2005**, *29*, 280−282.

(12) Wagner, B. D.; Stojanovic, N.; Day, A. I.; Blanch, R. J. *J. Phys. Chem. B* **2003**, *107*, 10741−10746.

(13) Plakhotnik, T.; Donley, E. A.; Wild, U. P. *Annu. Rev. Phys. Chem.* **1997**, *48*, 181−212.

JA073996N